Thermal annealing induced photocarrier radiometry enhancement for ion implanted silicon wafers*

Liu Xian-Ming(刘显明)[a)b)], Li Bin-Cheng(李斌成)[a)†], and Huang Qiu-Ping(黄秋萍)[a)b)]

[a)] *Institute of Optics and Electronics, Chinese Academy of Sciences, Chengdu* 610209, *China*
[b)] *Graduate School of the Chinese Academy of Sciences, Beijing* 100039, *China*

(Received 22 January 2010; revised manuscript received 23 February 2010)

An experimental study on the photocarrier radiometry signals of As^+ ion implanted silicon wafers before and after rapid thermal annealing is performed. The dependences of photocarrier radiometry amplitude on ion implantation dose (1×10^{11}–1×10^{16}/cm^2), implantation energy (20–140 keV) and subsequent isochronical annealing temperature (500–1100 °C are investigated. The results show that photocarrier radiometry signals are greatly enhanced for implanted samples annealed at high temperature, especially for those with a high implantation dose. The reduced surface recombination rate resulting from a high built-in electric field generated by annealing-activated impurities in the pn junction is believed to be responsible for the photocarrier radiometry signal enhancement. Photocarrier radiometry is contactless and can therefore be used as an effective in-line tool for the thermal annealing process monitoring of the ion-implanted wafers in semiconductor industries.

Keywords: photocarrier radiometry, ion implantation, thermal annealing, silicon
PACC: 7220J, 7855C, 7320H, 7340L

1. Introduction

Ion implantation is routinely used in semiconductor device manufacturing to modify the electrical properties of near surface regions of silicon wafers. In order to reduce the implantation-induced crystalline structural damage and activate the implanted ions, a subsequent thermal annealing process is indispensable.[1,2] As the scaling requirements for integrated circuit (IC) have become increasingly more and more stringent and difficult to achieve, the monitoring of the ion implantation and the annealing process is essential for fabricating the semiconductor devices.

As a dynamically modulated room-temperature photoluminescence technique, photocarrier radiometry (PCR) was introduced first by Mandelis and found to be a sensitive method of characterizing semiconductors and monitoring implantation dose.[3,4] In earlier papers, however, nearly all the PCR experiments were performed on the single-crystalline samples or ion-implanted samples without the thermal annealing process.[5−8] Further studies are necessary to know whether the PCR technique can be used to characterize the thermal annealed samples, or to evaluate the thermal annealing processes.

In the present study, the samples subjected to different ion implantation processes and different thermal annealing processes are investigated by photocarrier radiometry. Experimental results are presented and the effects of thermal annealing processes on the PCR signals are analysed in detail.

2. Experimental details

All substrates used in this work were prepared from the same batch of ⟨111⟩ oriented p-type Czochralski crystalline silicon wafers, (525±20 μm, 8–13 $\Omega\cdot$cm), with the front surface chemically-mechanically polished. Six groups of samples under different processing conditions were prepared. G1–G5 were implanted onto the polished surface with As^+ ions, and G6 was a group of substrates without implantation. As shown in Table 1, G1 and G2 were implanted with implantation doses from 1×10^{11} to 1×10^{16}/cm^2 at the same implantation energy of 100 keV. G3 and G4 were implanted with implantation energies from 20 to 140 keV at an implanta-

*Project supported by the National Natural Science Foundation of China (Grant No. 60676058).
†Corresponding author. E-mail: bcli@ioe.ac.cn
© 2010 Chinese Physical Society and IOP Publishing Ltd

tion dose of $1\times10^{15}/\text{cm}^2$. All samples of G5 were implanted with $1\times10^{15}/\text{cm}^2$ at 100 keV. After implantation, G1 and G3 were then annealed in a rapid thermal annealing (RTA) system for 30s at 1100° in an inert nitrogen atmosphere, and G2 and G4 were not annealed. G5 and G6 were annealed isochronically at various temperatures ranging from 500 to 1100° for 30s.

Table 1. List of sample groups under different implantation and annealing conditions.

group	implantation dose/(As^+/cm^2)	implantation energy/keV	annealing temperature/°C
G1	1×10^{11}–1×10^{16}	100	1100
G2	1×10^{11}–1×10^{16}	100	- -
G3	1×10^{15}	20–140	1100
G4	1×10^{15}	20–140	- -
G5	1×10^{15}	100	500–1100
G6	- -	- -	500–1100

The PCR experimental setup has been described in detail elsewhere.[7,8] Briefly, a 105 mW-power and 660 nm-wavelength semiconductor laser modulated by a function generator was used as an excitation source. A 10 nm-bandwidth bandpass filter centred at 660 nm was employed to block all unwanted radiation from the excitation source. The laser beam was focused onto the sample surface and the radius of the beam at the surface was measured to be approximately 20 μm. The infrared emissions from the samples, that is, the PCR signals, were collected and focused through a pair of off-axis paraboloidal mirrors onto an InGaAs detector (ThorLabs model PDA10CS, with a spectral response range from 700 to 1800 nm, and frequency bandwidth from dc to 17 MHz). An optical long-pass filter (with transmission $T < 0.1\%$ at 660 nm, $T > 73.5\%$ in 1000–1800 nm) was placed in front of the detector to block any leakage of the excitation source. The overall noise level of the setup was below 0.1 μV. For each silicon wafer, the frequency scan was performed at a total of 30 frequency points from 100 Hz to 600 kHz. The PCR signals from the detector were demodulated by a lock-in amplifier (Model 7280, Signal Recovery), with the amplitudes and phases recorded each as a function of modulation frequency. The experimental apparatus and the data acquisition were controlled by a computer with a Labview program.

3. Results and discussion

The ion implantation induces structural damage on the sample surface, which changes the optical reflectance. In order to compare the generated PCR signals under the same photon fluxes into the sample, the values of reflectance R of all samples at 660 nm were measured with a high-precision spectrophotometer (Lambda 900, Perkin Elmer). Then the PCR amplitudes were normalized by using the ratio of measured experimental data to value (1-R). Figure 1 shows the reflectances for samples with different (a) implantation doses, (b) implantation energies and (c) annealing temperatures. Here, the first data points in Fig. 1(c) are for the non-annealed (NA) samples.

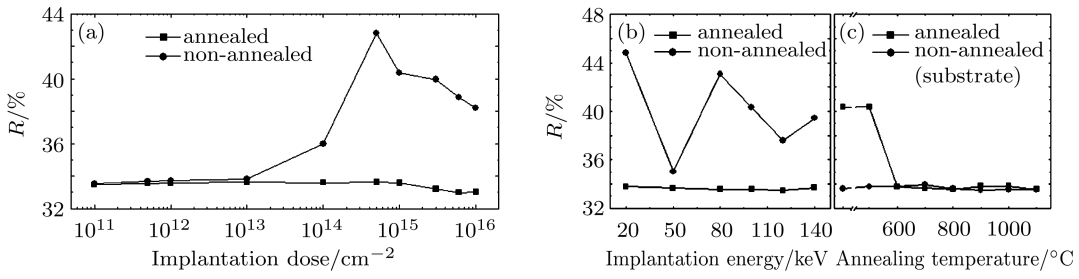


Fig. 1. Reflectances for samples with different (a) implantation doses, (b) implantation energies and (c) annealing temperatures. The first data points in (c) are for the non-annealed samples.

For samples without thermal annealing, the reflectances are related to implantation dose and energy. As the different implantation conditions induce various degrees of defects and damages, the optical properties of the implanted layer on the surface are complicated functions of implantation dose and energy, which are not analysed in this paper. The reflectances for annealed samples are lower than those without annealing. All the reflectances are approximately 33.6% for samples with annealing temperature above 600 °C, which is approximately equal to that of the sample without implantation. After thermal annealing, due to the recovery of the damaged structure during the high temperature annealing, the optical properties of the implanted layers in visible and near infrared ranges are close to those of the crystalline silicon as proven by spectroscopic ellipsometry (SE) data.[9]

Figure 2 shows the variations of PCR amplitudes for implanted samples with the increase of implantation dose, with and without the annealing process. The first data points are for the non-implanted (NI) samples. Since the PCR signal is more sensitive to the surface region at higher modulation frequency, only the signals in the kHz range are shown. The ion implantation into the crystalline silicon changed electrical and optical properties on the surface and the sub-surface region of the sample.[10] Shaughnessy *et al.* have shown that the PCR amplitude for a sample without annealing has a monotonic decrease over a large implantation dose range due to the implantation-induced damage,[4] which can also be found in our experiments. However, the tendency is totally opposite for annealed samples, which is shown in Fig. 2. For samples with high implantation doses, the high-temperature annealing process results in a strong increase of the PCR amplitude. Comparing the results obtained at 10 kHz, 100 kHz and 500 kHz, for annealed samples the sensitivities of PCR amplitudes to the implantation doses are approximately the same at different modulation frequencies. While for samples without annealing, the signals are more sensitive at higher modulation frequencies than at lower frequencies. However, the signals are faint at high modulation frequencies especially for samples with high implantation doses. Therefore, a moderate modulation frequency such as 100 kHz is more suitable for ion implantation dose monitoring for these non-annealed samples.

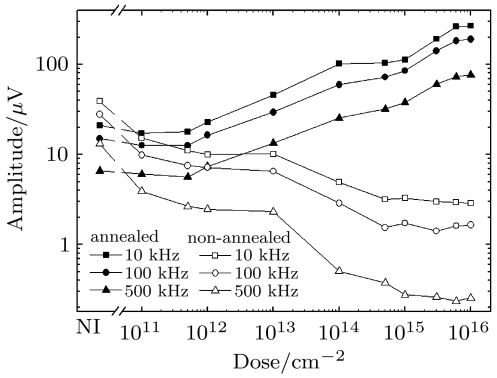


Fig. 2. PCR amplitudes versus ion implantation dose for samples G1 and G2, with and without annealing process. Amplitudes for non-implanted samples are presented as the first data points for comparison.

Figure 3 shows the variations of PCR amplitudes at different modulation frequencies for samples with implantation energy increasing, with and without the annealing process. The PCR amplitudes for both samples G3 and G4 each are a monotonic decreasing function of implantation energy. The amplitudes for annealed samples are much larger than those for corresponding non-annealed samples. Figure 4 shows the curves for PCR amplitude versus annealing temperature for samples G5 and G6, with and without implantation. Amplitudes for non-annealed samples are presented as the first data points for comparison. As shown in Fig. 4, the PCR signal enhancement factor largely depends on annealing temperature. The PCR amplitude for G5 increases monotonically with annealing temperature, and finally reaches a saturation level when the temperature exceeds 1000 °C. Meanwhile, for substrates G6 without implantation, the PCR amplitudes are approximately the same when the annealing temperature exceeds 600 °C.

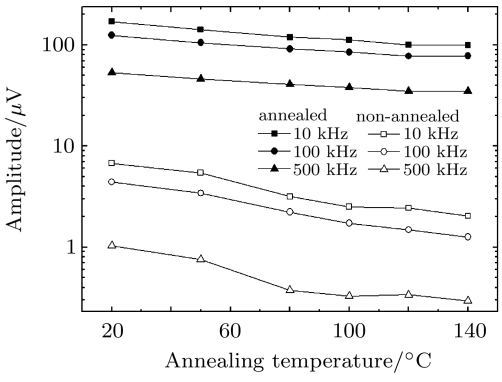


Fig. 3. PCR amplitudes versus ion implantation energy for samples G3 and G4, with and without thermal annealing process.

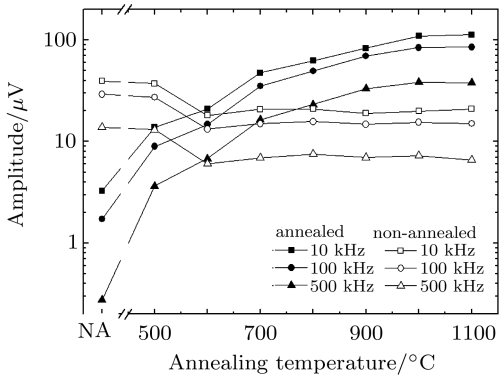


Fig. 4. PCR amplitude versus annealing temperature for samples G5 and G6, with and without implantation. Amplitudes for non-annealed samples are presented as the first data points for comparison.

PCR is a room-temperature photoluminescence technique. There have been several reports on the room-temperature luminescence of the ion implanted silicon wafers in the past few years.[11−18] Ng *et al.*[11] suggested that the ion implantation and the subsequent annealing process would induce dislocation loops in the samples, which might enhance the luminescence intensity. While Stowe *et al.*[13] found that the luminescence was independent of implanted layer, because the luminescence enhancement still existed even when the dislocations were removed by chemical etching. They proposed that gettering the effects of the dislocations due to ion implantation might be the reason for the luminescence enhancement. Basically, these models explained the room-temperature luminescence enhancement of silicon from the viewpoint of the microstructure of the annealed samples. Here, we propose an explanation for the photoluminescence enhancement or PCR signal enhancement based on the carrier transport model and a built-in electric field formed by both ion implantation and thermal annealing processes. From the PCR theory, the PCR amplitude is proportional to the photo-generated carrier density inside the sample, which is a function of electronic transport parameters, such as carrier lifetime, diffusion coefficient, and front surface recombination rate. When the samples are implanted with ions but not annealed, the damage to the lattice structure reduces the lifetime and the diffusion coefficient of carriers, and increases the surface recombination rate, resulting in the decrease of carrier concentration and therefore PCR amplitude.[4] A greater damage is introduced by higher implantation dose or energy, which causes the monotonic decreasing of the PCR amplitude with implantation dose and energy increasing as presented in Figs. 2 and 3 for non-annealed samples.

After the implanted samples are annealed at high temperatures, on the other hand, the structural damages induced by ion implantation are recovered and the implanted ions are activated to be effective electronic impurities. For the implanted samples subjected to high temperature annealing process, their optical properties in the visible and the near infrared ranges are recovered to be close to those of crystalline silicon[19] as already confirmed by the reflectance and SE measurements.[9,20] Meanwhile, for structurally intact substrates without implantation, the rapid temperature rising and falling in the thermal annealing process may induce thermal gradients in the wafer and give rise to thermoplastic stress. Defects such as dislocations and slip can come into being inside the substrates,[21] therefore decrease somewhat the PCR amplitudes. When the annealing temperature keeps increasing, higher temperature will induce more defects. However, the induced defects will be recovered at high temperature. The influence of high annealing temperature determines the concentration of the defects from two opposite sides, keeping approximately the defect concentration in balance when the temperature is higher than a critical value. The critical temperature is between 500 and 600 °C as shown in Fig. 4 for non-implanted samples. When the annealing temperature exceeds 600 °C, the effects of thermal annealing on PCR signals of substrates are approximately the same. Thus, the PCR signal enhancement with the increase of temperature for sample G5 is caused by the effects of both ion implantation and subsequent thermal annealing.

To evaluate the contribution of the implanted layer to the PCR signal, we calculate the average depth (vertical projected range) of implanted ions by TRIM software.[22] With the highest implantation energy of 140 keV, the depth of the implanted layer is 93.6 nm. After thermal annealing, the implanted layer attenuates only 2.8% of the pump laser power (absorption coefficient at 660 nm is 3.05×10^5 m^{-1} for crystalline silicon.[23]) Therefore, the PCR signals of implanted samples are mainly attributed to the photo-generated carriers within the substrate layer. As the lifetime and the diffusion coefficient of the carrier in the implanted layer have little influence on the PCR signal, the surface recombination rate is a main factor to determine the PCR amplitudes for annealed samples.

For implanted and annealed samples, the acti-

vated ion-implanted layer (with As^+, n-type) and the substrate layer (with B^+, p-type) form a pn junction at the interface between the two layers. An electric field is created in the space charge region due to the separation of positive charges from negative space charges.[24,25] The electric field is determined by the product of carrier (hole and electron) concentrations in both p and n regions. Higher carrier concentration results in a stronger electric field. In our experiments, the hole concentrations in p regions are the same for all implanted wafers. In n regions, on the other hand, the electron concentrations are equal to the concentrations of effective impurities which are the activated implanted ions. The electric field produces a force acting on the holes and electrons to block them from diffusing into the other side. Therefore, few carriers in the bulk region of the substrate can go through the electric field and the implanted layer. Most of the carriers may not recombine at the front surface of the sample but at the interface between the implanted layer and the substrate, that is, the surface of the substrate layer. The probability of surface recombination is therefore substantially reduced due to the existence of the internal electric field.[26] As a special case of Shockley–Read-Hall (SRH) recombination, surface recombination is an important mechanism of non-radiative recombination.[27] If the surface recombination is suppressed, more electron–hole pairs will recombine directly by radiative band-to-band or band-to-impurity recombination. The concentrations of the free carriers for radiative recombination are significantly enhanced. As a result, the PCR amplitudes or the luminescence intensities are greatly enhanced as well.

When the samples are implanted with the same energies, the thicknesses of the implanted layers are approximately the same for different implantation doses. More implanted ions can be activated under the same annealing conditions for samples with higher implantation doses, resulting in stronger built-in electric fields, and therefore more enhanced PCR signals. This explains well the dependence of the PCR amplitude on dose as shown in Fig. 2. When samples are implanted with the same implantation doses, shallower junctions are formed with a lower implantation energy, resulting in a higher impurity concentration and a stronger electric field. Therefore, the PCR amplitude decreases with the increase of implantation energy as shown in Fig. 3. Annealing temperature is another factor to determine the concentration of the effective impurities. More implanted impurities can be activated at high temperatures, resulting in larger PCR amplitudes as shown in Fig. 4. The amplitude begins to saturate at an annealing temperature of 1000 °C, which represents the critical temperature, above which the implanted impurities are totally activated.

It is worth mentioning that the electric field is not only formed in a pn junction. When the substrate of p-type (or n-type) is doped with impurities of the same type of electric properties, a pp^+ (or nn^+) junction is formed.[26] There are also electric fields in these junctions, which affect the surface recombination rate and the PCR signals as well. So the room-temperature luminescence of sample with or without pn-junction in Ref. [12] can be well explained by the reduction of surface recombination rate due to built-in electric fields. On the other hand, for samples with Si^+ ions implantation, no luminescence enhancement can be found, as Si^+ ions are not effective electric impurities and no electric field is formed.[12]

4. Conclusion

The presented experimental results show that for ion-implanted and thermally annealed silicon wafers, the PCR signal is sensitive not only to the implantation induced damage, but also to the annealing activated impurity concentration. The PCR technique is demonstrated to be a useful tool for both ion implantation and thermal annealing monitoring. Furthermore, the analytical model for PCR enhancement may be helpful for designing and fabricating silicon-based room-temperature light-emitting devices.

References

[1] O'Mara W C, Herring R B and Hunt L P 1990 *Handbook of Semiconductor Silicon Technology* (Park Ridge: Noyes Publications)

[2] Quirk M and Serda J 2001 *Semiconductor Manufacturing Technology* (Beijing: Pearson Education)

[3] Mandelis A, Batista J and Shaughnessy D 2003 *Phys. Rev.* B **67** 205208

[4] Shaughnessy D, Li B, Mandelis A and Batista J 2004 *Appl. Phys. Lett.* **84** 5219

[5] Batista J, Mandelis A and Shaughnessy D 2003 *Appl. Phys. Lett.* **82** 4077
[6] Li B, Shaughnessy D, Mandelis A, Batista J and Garcia J 2004 *J. Appl. Phys.* **95** 7832
[7] Shaughnessy D and Mandelis A 2006 *J. Electrochem. Soc.* **153** G283
[8] Liu X, Li B and Zhang X 2008 *J. Appl. Phys.* **103** 123706
[9] Lioudakis E, Christofides C and Othonos A 2006 *J. Appl. Phys.* **99** 123514
[10] Nastasi M and Mayer J W 2006 *Ion Implantation and Synthesis of Materials* (Berlin: Springer-Verlag)
[11] Ng W L, Lourenço M A, Gwilliam R M, Ledain S, Shao G and Homewood K P 2001 *Nature* **410** 192
[12] Stowe D J, Galloway S A, Senkader S, Mallik K, Falster R J and Wilshaw P R 2003 *Physica* B **340–342** 710
[13] Stowe D, Fraser K, Galloway S, Senkader S, Falster R and Wilshaw P 2006 *Microscopy of Semiconducting Materials: Proceedings of the 14th Conference* Oxford, UK, 11–14 April, 2005 p355
[14] Lourenço M A, Milosavljević M, Shao G, Gwilliam R M and Homewood K P 2006 *Thin Solid Films* **504** 36
[15] Yuan Z, Li D, Gong D, Wang M, Fan R and Yang D 2007 *Mat. Sci. Semicon. Proc.* **10** 173
[16] Yuan Z, Li D, Wang M, Gong D, Fan R and Yang D 2008 *Vacuum* **82** 1337
[17] Sobolev N, Emel'yanov A, Sakharov V, Serenkov I, Shek E and Tetel'baum D 2007 *Semiconductors* **41** 537
[18] Huang W Q, Xu L, Wang H X, Jin F, Wu K Y, Liu S R, Qin C J and Qin S J 2008 *Chin. Phys.* B **17** 1817
[19] Pelaz L, Marqués L and Barbolla J 2004 *J. Appl. Phys.* **96** 5947
[20] Liu X M, Li B C, Gao W D and Han Y L 2010 *Acta. Phys. Sin.* **59** 1632 (in Chinese)
[21] Campbell S A 2001 *The Science and Engineering of Microelectronic Fabrication,* 2nd edition (Beijing: Publishing House of Electronics Industry) p137
[22] Ziegler J F, Biersack J P and Littmark U 1985 *The Stopping Range of Ions in Solids* (Tarrytown, NY: Pergamon); Ziegler J F http://www.srim.org [2006-]
[23] Palik E D 1998 *Handbook of Optical Constants of Solids* (San Diego: Academic)
[24] Colinge C A and Colinge J-P 2002 *Physics of Semiconductor Devices* (New York: Kluwer Academic Publishers)
[25] Mishra U K and Singh J 2008 *Semiconductor Device Physics and Design* (Netherlands: Springer)
[26] Rein S 2005 *Lifetime Spectroscopy* (Berlin: Springer-Verlag)
[27] Yacobi B G 2003 *Semiconductor Materials* (New York: Kluwer Academic Publishers)